Design of Novel Dielectric Surface Modifications for Perylene Thin-Film Transistors

Christian Effertz, Stefan Lahme, Philip Schulz, Ingolf Segger, Matthias Wuttig, Arno Classen, and Carsten Bolm*

Dielectric surface modifications (DSMs) can improve the performance of organic thin-film transistors (OTFTs) significantly. In order to gain a deeper understanding of this performance enhancement and to facilitate high-mobility transistors, perylene based devices utilizing novel dielectric surface modifications have been produced. Novel DSMs, based on derivates of tridecyltrichlorosilane (TTS) with different functional end-groups as well as polymeric dielectrics have been applied to tailor the adhesion energy of perylene. The resulting samples were characterized by electronic transport measurements, scanning probe microscopy, and X-ray diffraction (XRD). Measurements of the surface free energy of the modified dielectric enabled the calculation of the adhesion energy of perylene upon these novel DSMs by the equation-of-state approach. These calculations demonstrate the successful tailoring of the adhesion energy. With these novel DSMs, perylene thin-films with a superior film quality were produced, which enabled high-performance perylene-based OTFTs with high charge-carrier mobility.

1. Introduction

Organic electronics have entered everyday life as organic light-emitting diodes (OLEDs) and can nowadays be found in a variety of applications.[1] While OLEDs have accomplished the step from basic research to market readiness with sales exponentionally growing and exceeding $ 1B in 2008, organic thin-film transistors (OTFTs) still lag behind. Nevertheless, they are intensively studied as the material of choice in flexible active matrix devices or in low-cost radio-frequency-identification (RFID) tags.[2–4] One of the reasons for the absence of commercial organic thin-film transistor applications is their slow switching speed due to the low charge-carrier mobility. While recent reports indicate that organic single crystals can match hydrogenated amorphous silicon (a-Si:H) in terms of mobility, most OTFTs are based on inexpensive processable thin films, which show significantly lower charge-carrier mobilities.[2,5] Hence it is important to tailor the film-formation process to produce high-mobility OTFTs. Dielectric surface modifications represent a potentially rewarding route towards high-performance OTFTs.

It has been shown that the mobility and I_{ON}/I_{OFF} ratio of organic field-effect transistors can be improved by modifying the dielectric.[6–10] The I_{ON}/I_{OFF} ratio is directly influenced by the mobility, as a high charge-carrier mobility will lead to a large current at a given voltage. In the following we will summarize the improvement of the mobility and the I_{ON}/I_{OFF} ratio as the performance enhancement, since the characteristics of a transitor device depend crucially on these two. However, one has to note that the performance of the full device also depends on other quantities, such as the transitor's geometry as well as production and operation parameters.

Potential dielectric modifications include but are not limited to polymeric organic adlayers such as poly(vinylphenol) (PVP), solution-processed self-assembled monolayers (SAMs) such as octadecyltrichlorosilane (OTS) or vapor-phase processed SAM molecular gate dielectrics.[6–12] In some of these publications the improvement of the charge-carrier mobility and the I_{ON}/I_{OFF} ratio has already been related to the surface free energy (SFE) of the dielectric surface modification (DSMs. A detailed review on the research of dielectric surface modifications can be found, for example, in a previous report.[13] What has been lacking is a quantitative evaluation of the correlation between adhesion energy and charge-carrier mobility. To establish this relationship it is mandatory to tailor the adhesion energy of the organic film and the DSM. This is the goal of this study.

2. Results and Discussion

To tackle this task and in order to systematically study the influence of dielectric surface modifications, DSMs are needed that lead to a clearly distinguishable adhesion energy of the perylene film. Most desirable would be a DSM leading to a low adhesion energy, a DSM leading to a high adhesion energy, and a DSM leading to an intermediate-adhesion energy. The three

Dr. C. Effertz, S. Lahme, P. Schulz, I. Segger, Prof. M. Wuttig
Physikalisches Institut (IA)
RWTH Aachen University
52056 Aachen, Germany
E-mail: effertz@physik.rwth-aachen.de
A. Classen, Prof. C. Bolm
Institut für Organische Chemie
RWTH Aachen University
52056 Aachen, Germany

DOI: 10.1002/adfm.201101299

cases are defined in relation to the cohesive energy of perylene, which we have determined by contact-angle measurements on perylene thin films to (50.3 ± 3.0) mN m^{-1}. Hence, we have been choosing three DSMs with adhesion energies significantly higher, smaller, and close to 50.3 mN m^{-1}. In case of polymeric dielectrics, DSMs fulfilling these requirements can easily be found, as a large variety of polymers have already been studied regarding their SFE in the past.[14] For a known SFE, which is measureable, e.g., by contact-angle measurements, the adhesion energy can be calculated as a function of the SFE of the substrate ($\gamma_{substrate}$) and the perylene layer ($\gamma_{perylene}$):

$$E_{adh}^{substrate,\ perylene} = E(\gamma_{substrate}, \gamma_{perylene}). \quad (1)$$

To find suitable DSMs, in case of polymeric dielectrics, commercially available compounds were chosen, the SFE of the polymeric dielectric produced was measured, and the adhesion energy was calculated. In this study, the polymeric dielectrics poly-(dimethylsiloxane) (PDMS), polystyrene (PS), and poly(-methylmethacrylate) (PMMA) were chosen. In the case of SAMs, the number of commercially available compounds that have been proven to be suitable for OTFT production of SiO_2 is limited. OTS is a popular representative of self-assembling molecules and leads to a mobility enhancement in perylene TFTs by up to three orders of magnitude.[9] It was shown that the adhesion energy of perylene on OTS is lower than the cohesive energy (E_{adh} = (44.3 ± 1.3) mN m^{-1} < (50.3 ± 3.0) m N m^{-1}).[10] Hence, to facilitate our attempt to study perylene TFTs produced on low, high, and mid-adhesive dielectrics, novel SAMs are needed.

Phenyltridecyltrichlorosilane (PhenylTTS) and naphtyltridecyltrichlorosilane (NaphtylTTS) are novel molecules designed and synthesized in-house for the formation of SAMs. Similar to OTS, these molecules consist of a $SiCl_3$ group, which leads to the chemisorption of the molecule on the SiO_2 surface. The other end of the tridecyl chain ($(CH_2)_{13}$) is terminated by phenyl (C_6H_5) or naphthyl ($C_{10}H_7$), in contrast to methyl (CH_3) in the case of OTS. The different endgroups were applied to systematically tailor the surface free energy of the SAM formed and thus to control the perylene adhesion. The SFE can be partitioned into contributions from polar and dispersive dipole interactions. Strong permanent dipoles lead to a large polar contribution to the SFE. A high polarizablity leads to large dispersive contribtuions to the SFE. As a change in the endgroup influences the strength of permanent dipoles as well as the polarizability of the SAM molecule, the SFE is changed in turn.[15] We have assumed that the phenyl endgroup leads to a higher SFE than the methyl termination of OTS and that the naphthyl endgroup leads to an even higher SFE. This assumption is based upon both calculations of the static dipole moment with Gaussian 09, using B3LYP functionals, and upon the approximation of the strength of the dispersive dipoles. The calculations yield only a minor increase of the static dipole moment from 2.9 Debye (OTS and PhenylTTS) to 3.1 Debye (NaphtylTTS). However, by changing from σ-bound methyl to π-rich systems, such as phenyl and naphthyl, the polarizability and hence the dispersive dipole moment is increased. This should lead to a larger SFE, as will be confirmed below. By designing DSMs with a tailored SFE the adhesion energy of perylene is controled.

Table 1. SFE and adhesion energy calculated from contact-angle measurements on the DSM and on the unmodified dielectric, average and best measured mobility of the OTFTs, and normalized maximum intensity and FWHM of the rocking curve scans of perylene thin-films. The error reported for the average mobility is the standard deviation, while the error reported for the best mobility is the standard error originating from linear fitting. By designing and synthesizing novel SAMs the adhesion energy of perylene has been controlled with pronounced consequences for the charge-carrier mobility μ, as revealed by the correlation between the mobility and the adhesion energy. Low-adhesive DSMs such as PDMS and OTS lead to superiour device performance, followed by mid-adhesive DSMs such as PS and PhenylTTS. High-adhesive DSMs PMMA and NaphthylTTS lead to a device performance only one order of magnitude better than the reference sample. XRD results indicate that highly textured films with good crystall quality can be grown on low-adhesion DSMs. The maximum intensity of the (001) peak of the α-structure of perylene is given in units normalized in respect to the reference sample.

Modification	SFE [mN m^{-1}]	E_{adh} [mN m^{-1}]	Av. μ [cm^2 V^{-1}s^{-1}]	Best μ [cm^2 V^{-1}s^{-1}]	Max. Int.	FWHM
PDMS	19.7 ± 0.6	44.3 ± 1.4	(2.8 ± 0.9) · 10^{-2}	(3.9 ± 0.1) · 10^{-2}	57.2	0.3°
PS	30.9 ± 0.6	54.6 ± 1.8	(5.2 ± 0.7) · 10^{-3}	(6.1 ± 0.1) · 10^{-3}	5.3	1.3°
PMMA	40.0 ± 0.7	61.7 ± 2.2	(7.9 ± 0.4) · 10^{-4}	(8.6 ± 0.1) · 10^{-4}	2.5	2.0°
OTS	19.7 ± 0.5	44.3 ± 1.3	(1.4 ± 0.4) · 10^{-2}	(1.9 ± 0.1) · 10^{-2}	37.7	0.1°
PhenylTTS	28.5 ± 0.8	53.4 ± 1.7	(5.0 ± 3.0) · 10^{-3}	(9.1 ± 0.1) · 10^{-3}	10.1	1.1°
NaphthylTTS	30.3 ± 3.0	55.1 ± 3.1	(3.2 ± 0.1) · 10^{-4}	(5.0 ± 0.1) · 10^{-4}	2.5	1.6°
Reference	55.9 ± 0.9	66.6 ± 2.8	(2.7 ± 1.0) · 10^{-5}	(4.1 ± 0.1) · 10^{-5}	1	2.2°

Table 1 summarizes the results of the surface free energy and adhesion energy as calculated from contact-angle measurements. By the application of different polymeric dielectrics and SAMs we have aimed at facilitating low, intermediated and high-adhesion DSMs. As expected, PDMS has the lowest adhesion energy with perylene out of all investigated polymeric dielectrics ((44.3 ± 1.4) mN m^{-1}) followed by PS ((54.6 ± 1.8) mN m^{-1}) and PMMA ((61.7 ± 2.2) mN m^{-1}). For SAMs, the adhesion energy increases from OTS ((50.3 ± 3.0) mN m^{-1}) over PhenylTTS ((53.4 ± 1.7) mN m^{-1}) to NaphthylTTS ((55.1 ± 3.1) mN m^{-1}), which is still smaller than the adhesion energy of perylene on SiO_2 ((66.6 ± 2.8) mN m^{-1}). Hence, the contact-angle measurements confirm the success of our design strategy: as aimed for, the adhesion energy of perylene on NaphthylTTS is higher than the adhesion energy for PhenylTTS, which in turn is higher than the adhesion energy of OTS. By comparing the calculated adhesion energies with the cohesive energy of perylene, which is ((50.3 ± 3.0) mN m^{-1}), PDMS for polymeric dielectrics and OTS for SAMs lead to a perylene adhesion energy lower than the cohesive energy. PMMA and NaphthylTTS, on the contrary, lead to a perylene adhesion energy higher than the cohesive energy. Perylene films on PS and PhenylTTS have an adhesion energy ranging in between these two extrema. Hence, by the application of PhenylTTS and NaphthylTTS the adhesion properties of perylene by dielectric surface modifications is tailored. All adhesion energies are lower than the adhesion energy of perylene on unmodified SiO_2.

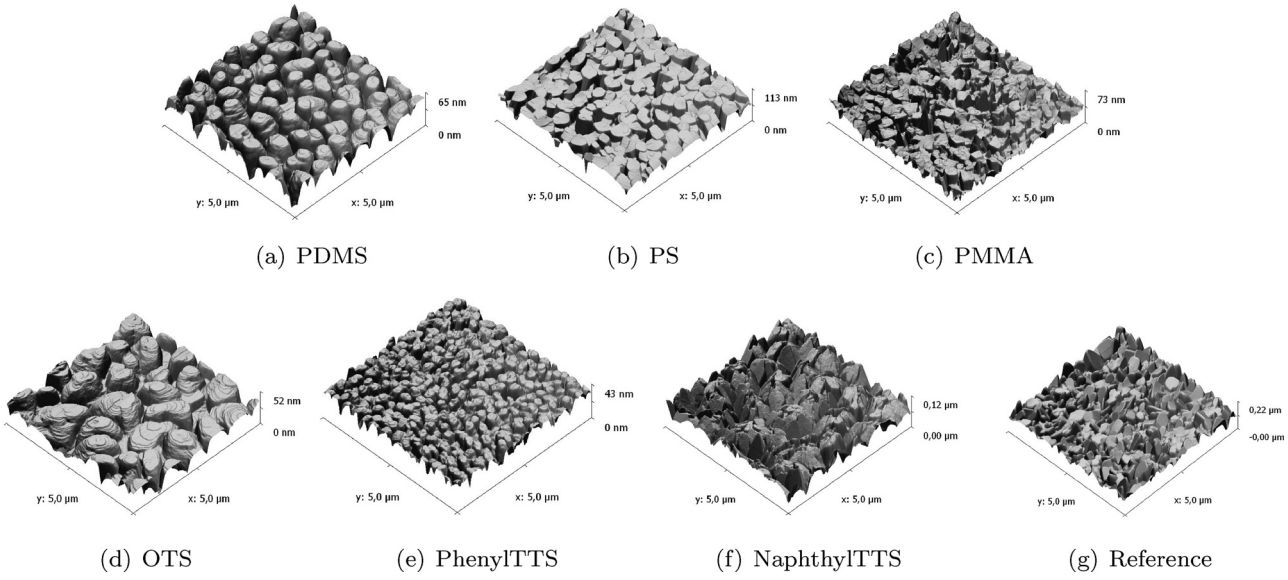

Figure 1. AFM scans obtained in tapping mode - the application of DSM and the related change of adhesion energy influences thin-film growth and thus the morphology. One can clearly see that low- and intermediate-adhesion DSMs lead to uniformly shaped grains with a prevailing growth direction perpendicular to the substrate surface. High-adhesion DSMs lead to an irregular growth as also observed for the reference sample. By comparing the low-adhesion DSMs PDMS and OTS with intermediate-adhesion DSMs PS and PhenylTTS, one can see that a lower adhesion energy leads to larger grains.

The influence of the DSM on the morphology of the perylene films is clearly visible in **Figure 1**. Films grown on PDMS, PS, OTS, and PhenylTTS show large regular-shaped grains with almost no inclination with respect to the substrate surface. The growth direction is uniformly parallel to the surface normal. Films on PMMA, NaphthylTTS, and unmodified SiO_2 show irregular-shaped grains with an inhomogeneous size distribution. The individual grains are not growing uniformly perpendicular to the substrate surface but show a pronounced inclination with respect to the substrate surface.

In addition to AFM, X-ray scans were performed in Bragg–Brentano ($\theta - 2\theta$) and rocking-curve geometry. The crystalline quality of the perylene films is correlated to the maximum intensity of the (001)-peak and the full-width at half maximum (FWHM) of the corresponding rocking curve.

The pronounced inclination of the grains that was observed by AFM is confirmed by XRD. The FWHM of the rocking curves measured in the (001)-diffraction peak of perylene (see Table 1) show: While perylene films on PDMS and OTS lead to narrow rocking curves, a distinct broadening can be observed for films on PMMA, NaphthylTTS, and in the case of the reference sample. XRD scans carried out in Bragg–Brentano show that thin films on PDMS and on OTS have the highest crystallinity and all samples containing a DSM have a higher crystallinity than thin films grown on unmodified SiO_2.

The large difference in film perfection can now be explained with the film formation process: Two different parameters govern the formation of the perylene thin film upon the modified substrate, namely the arrival of the molecules perylene rate and their diffusivity.[12] In our case, the depositon rate is constant for all samples. The diffusivity will change with temperature and with the adhesion energy of the evaporated material on the substrate surface. Since the substrate temperature is kept constant, film formation is governed by the adhesion energy. In general, if the adhesion energy is high, the diffusion of molecules on the surface is reduced, which leads to a small mean-free-path and the formation of smaller islands. If the adhesion energy is low, the diffusion of the molecules is more pronounced leading to a larger mean free path and the formation of larger islands.

If the adhesion energy of the perylene molecules on the substrate is higher than their cohesion energy, during the growth of the first monolayers, perylene molecules are more likely to stick to the surface rather than clustering to each other. This leads to a perturbation of film formation in the first monolayers. With increasing film thickness, the influence of the substrate vanishes, but arriving molecules form islands on the perturbed base layers. This is indicated by a large variation of growth direction as seen by broad XRD rocking curves and tilted islands as seen in the AFM scans in the case of perylene films grown on PMMA, NaphthylTTS, and on unmodified SiO_2. If the adhesion energy is lower than the cohesion energy, bulk-like growth is initiated from the first layer leading to the regular formation of highly crystalline grains. These grow perpendicular to the substrate as can be seen in the case of PDMS and OTS. Hence, using the DSMs with tailored adhesion energy for perylene enables the growth of thin-films with superiour film quality.

Table 1 shows the results of all transistor measurements. Transfer characteristics of the best TFTs on every DSM are shown in **Figure 2**a and b. For transistors both on polymeric dielectrics as well as on SAMs, a clear correlation between the adhesion energy and the device performance can be observed, as depicted in **Figure 3**. A low-adhesion energy leads to a high mobility and hence a good device performance. In particular, Figure 2b shows that the novel dielectric surface modifications

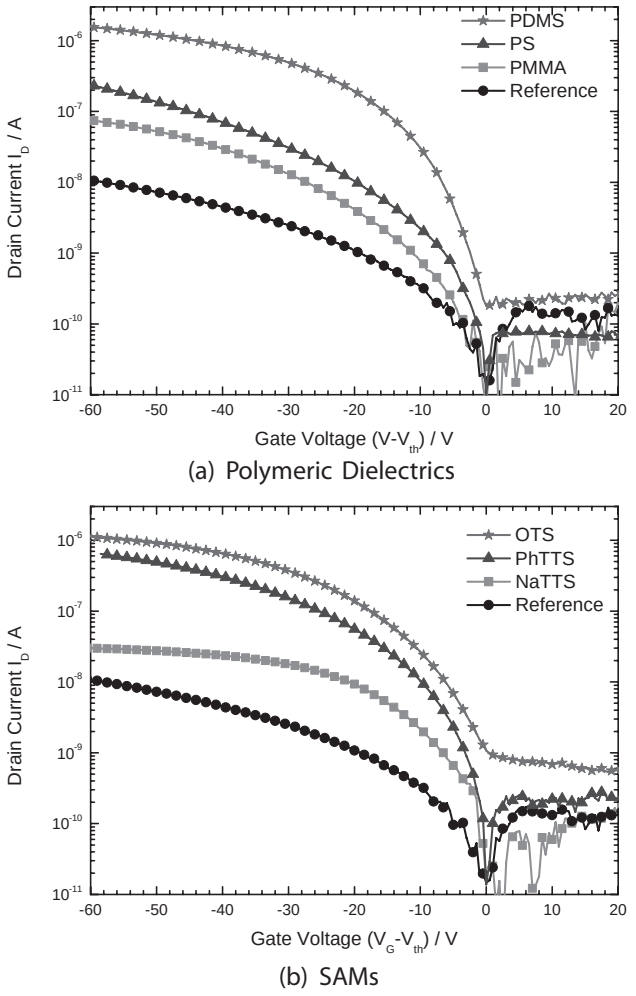

Figure 2. Transfer characteristics for different dielectric surface modifications: polymeric dielectrics (a) and SAMs (b). For better comparison, the drain current is plotted with respect to the gate voltage reduced by the threshold voltage ($V_G - V_{th}$). The threshold voltages are +6 V, −35.5 V, and −15.5 V for PDMS, PS, and PMMA respectively; and −2.5 V, −41.5 V, −3 V, and −33 V for OTS, PhenylTTS, NaphthylTTS, and the Reference. The shift in threshold voltage is attributed to the change in trap-state density in the perylene film and at the DSM/organic interface.[19–21] The subthreshold slopes are 3.22 V dec^{-1}, 4.35 V dec^{-1}, and 6.67 V dec^{-1} for PDMS, PS, and PMMA; and 2.86 V dec^{-1}, 2.70 V dec^{-1}, 9.10 V dec^{-1}, and 16.67 V dec^{-1} for OTS, PhenylTTS, NaphthylTTS, and the Reference.

PhenylTTS and NaphthylTTS are suitable for perylene TFT production since they, as all TFTs produced on DSMs, outperform TFTs produced on standard SiO_2. OTFTs on the low-adhesion DSMs, PDMS, and OTS, show an average mobility three orders of magnitude higher than standard OTFTs. Transistors on the mid-adhesion DSMs PS and PhenylTTS exhibit a mobility that is at least two orders of magnitude higher than the one observed for standard OTFTs. Even in the case of OTFTs on high-adhesion DSMs such as PMMA and NaphthylTTS still an increase of mobility of one order or magnitude can be observed. In conclusion, carefully designed dielectric surface modifications show a similar performance enhancement potential as polymeric dielectrics. The designed SAMs can be utilized in particular to meet the application requirements, e.g., a specific

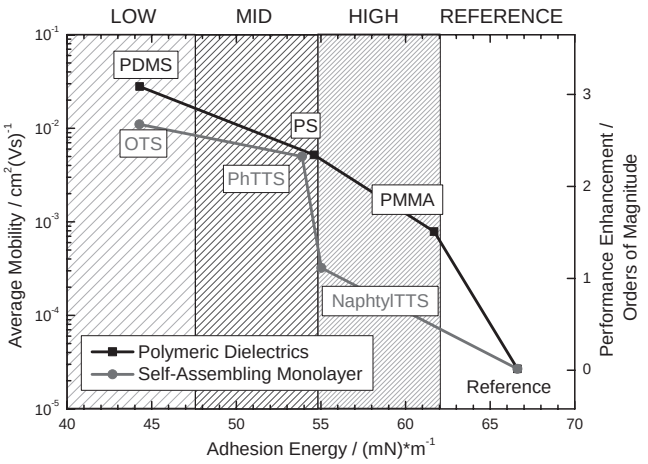

Figure 3. DSMs can be partitioned into three different classes: low-adhesion, intermediate/mid-adhesion and high-adhesion DSMs. By appling high-adhesion DSMs, the mobility is enhanced by one order of magniture in comparison to the reference. By appliying intermediate-adhesion DSMs, a mobility enhancement of another order of magnitude is found. OTFTs based on low-adhesion DSMs show a performance enhancement of three orders of magnitude in comparison to the reference sample.

adhesion energy. By substituting the $SiCl_3$ end group by other groups the design of DSMs applicable for a specific substrate is enabled. For example, by substituting $SiCl_3$ by a thiole group (R–S–H), SAMs, which were designed for the application on silicon dioxide, can be applied to gold surfaces. Hence, by the design of novel SAMs literally every active layer molecule can be paired with a large variety of substrates.

The investigation of the film morphology and the crystal quality of perylene thin-films grown on different DSMs indicate that the enhancement of the OTFT performance is correlated to the improvement of the film perfection. However, by applying different DSMs, the electronic structure of the dielectric/organic interface is influenced as well. This can lead to a change in interfacial trap-state density and distribution, which might provide an alternative explaination for the mobility evolution. However, a change in the trap-state density and distribution should lead to a shift in the threshold voltage and hence will be visible from the OTFT's transfer characteristics.[6,13,19–21] In case of the OTFT characteristics measured, the threshold voltages are +6 V, −35.5 V, and −15.5 V for PDMS, PS, and PMMA, respectively; and −2.5V, −41.5V, −3V, and −33V for OTS, PhenylTTS, NaphthylTTS, and the Reference. Hence, one can conclude that different DSMs indeed lead to a different trap-state density and distribution as indicated by different threshold voltages. However, no clear correlation between the threshold voltage and the charge-carrier mobility can be seen. Therefore, the improvement of the device performance, as defined in the introduction, is not governed by a change in the trap state density but instead the dominating influence stems from the adhesion energy.

3. Conclusion

In conclusion, by the application of novel organic adhesives as dielectric surface modifications, organic thin-film transistors

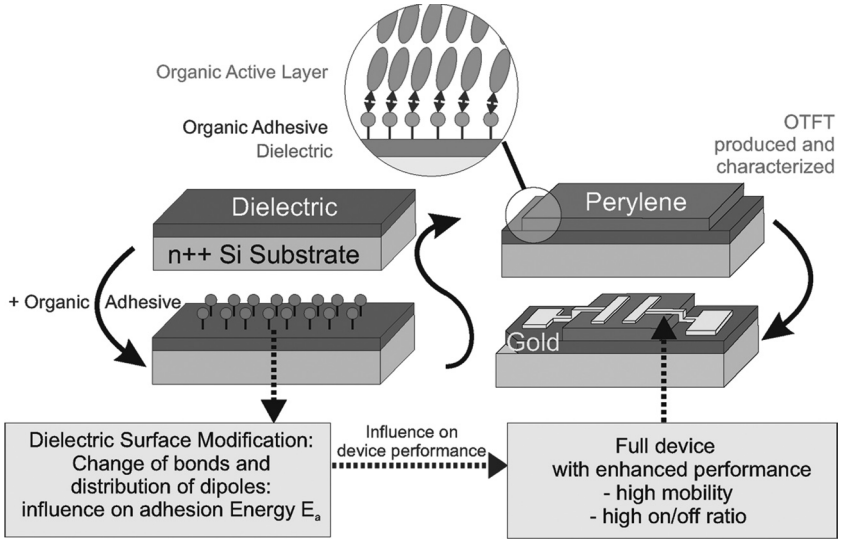

Figure 4. Sketch of the OTFT layout and production steps. At first, the substrate, which consists of a highly doped silicon wafer covered with thermally grown silicon dioxide is cleaned. In a next step, the DSM, which is an organic adhesive, is applied. The DSM acts as an intermediary between the silicon dioxide surface and the organic active layer. The electronic configuration as well as the dipole strength of the DSM determines the energetic landscape on which the perylene thin-film is formed. The active layer, perylene in our case, is deposited on the modified dielectric via physical vapor deposition (PVD). To finalize the transistor, gold contacts are applied by PVD through a shadow mask. By an appropriate choice of DSM OTFTs with high mobility and a high on/off ratio can be prepared.

have been produced that are capable of outperforming transistors on standard silicon dioxide. To achieve this goal, novel DSMs were employed, which possess a carefully selected surface free energy that helps tailor the adhesion energy of perylene. With these DSMs, perylene thin-films with superiour film quality were produced. A clear correlation between the adhesion energy and the charge-carrier mobility has been demonstrated.

4. Experimental Section

A schematic of the production procedure of an organic thin-film transistor is depicted in **Figure 4**. A highly n-doped silicon substrate acts as gate contact, while 600-nm thermally grown SiO_2 forms the basic dielectric. Prior to the perylene film deposition, all samples were cleaned with acetone and 2-propanol in an ultrasonic bath for 15 min each. Subsequently, dielectric surface modifications were processed in further production steps.

PhenylTTS was synthesized by a 6-step reaction sequence starting from 1,12-dodecandiol. Treatment with 48% HBr followed by copper-catalyzed carbon chain extension of the resulting intermediate with benzylmagnesiumchloride afforded the C13 alcohol with terminal hydroxyl and phenyl groups. Mesylation and subsequent Finkelstein reaction gave 13-phenyltridecylbromide. Dehydrohalogenation with K-tert.-butanolate/18-crown-6 followed by platinum-catalyzed hydrosilylation of the resulting olefin with trichlorosilane produced the desired compound in 47% overall yield.

An 8-step reaction sequence starting from 1,12-dodecandiol was developed for the synthesis of NaphthylTTS. In this case, the diol was treated with 48% HBr followed by THP-protection of the hydroxyl group and phosphonium salt formation with triphenylphosphine. Sequential Wittig reaction with 1-naphthaldehyde, acidic deprotection and hydrogenation with Pd/C gave 13-(1-naphthyl) tridecylalcohol. Finally, an analogous sequence as described for PhenylTTS led to NaphthylTTS in 26% overall yield.

PhenylTTS and NaphthylTTS are processed by immersion as commonly used for the production of OTS monolayers. PhenylTTS and NaphthylTTS are solved in dry hexane (<0.02% H_20) at a ratio of 1: 250, OTS in the ratio 1: 2500. The cleaned substrates for TFT production are placed into a beaker filled with the solvent for 1 h. After the immersion time, the samples were rinsed with hexane and dried at ambient air.

PS and PMMA are solved in ultrapure (>99%) chlorobenzene at a (mass) ratio of 1: 33, PDMS is solved at a ratio of 1: 50 in 2-propanol. In the case of PDMS, 170 µL of the solution is dropped on the cleaned SiO_2 surface. After 5 min of immersion, in which the molecules form a film on the surface, the samples were rotated in a spincoater at high rotation frequency in order to remove excess liquid. Subsequently, the samples were placed into an oven at 433 K for 1 h in order to remove the last residua of the solvent. DSMs of PS and PMMA are produced in a similar way, 500 µL of the solution is dropped on the SiO_2 surface followed by instant spin-coating without immersion time. The samples are heated in an oven at 363 K for 1 h. For comparison, OTFTs on an unmodified dielectric (in the following and above refered to as "reference") were produced as well.

In order to evaluate the surface free energy of the modified dielectric and the adhesion energy of perylene on the DSM, contact-angle measurements were performed using a Krüss DSA10. Contact angles of water, glycerol, ethylene glycol, diethyleneglycol and 2,2'-thiodiethanol were measured and used to calculate the SFE and the adhesion energy using the equation of state approach based on "Berthelots rule". Hereby, the contact angles Θ_l obtained for the different liquids and the knowledge of the surface tension of the respective liquid (γ_l) are used to calculate the SFE (γ_s). To do so, the values for $(1 + \cos(\Theta_l))$ obtained from contact-angle measurements with the different liquids are plotted against γ_l. Then, by following the equation of state approach,

$$(1 + \cos(\Theta_l)) = 2\sqrt{\gamma_l \gamma_s} \cdot \exp(-\beta \cdot (\gamma_l - \gamma_s)^2) \quad (2)$$

with the emperical constant $\beta = 1.247 \cdot 10^{-4}$ m^4 mJ^{-2}, the independent variable γ_s is fitted to the data. The adhesion energy between two phases, e.g., DSM and perylene thin-film can be calculated by

$$E_{ad_{i,j}} = 2\sqrt{\gamma_i \gamma_j} \cdot \exp(-\beta \cdot (\gamma_i - \gamma_j)^2) \quad (3)$$

In case of $i = j$, Equation 3 gives the cohesive energy.[14]

Perylene thin-films were produced by PVD at a base pressure of 10^{-7}mbar and a substrate temperature of 293 K. The growth rate was kept constant at 0.38 nm s^{-1} until a film thickness of 280 nm was reached. The film morphology was determined by atomic force microscopy (AFM).

To produce working OTFTs, gold electrodes were evaporated by PVD on top of the perylene film, while the sample was kept at a constant temperature of 278 K. The electrical characterization was performed using a Keithley 4200-SCS semiconductor analyzer. Transfer characteristics of up to 14 TFTs produced on one substrate were measured at a constant drain voltage $V_D = -20$ V by sweeping the gate voltage between 40 V and –120 V in steps of 0.5V.

The mobility is extracted from the saturation regime of the OTFTs transfer characteristics. In the saturation regime ($V_G - V_T \geq V_D$), the drain current is independent of the drain voltage:

$$I_D = \frac{1}{2}\mu C_{ox} \frac{W}{L} (V_G - V_T)^2 \quad (4)$$

Here, C_{ox} is the capacity of the dielectric per unit area, W is the channel width (i.e., the parallel length of the electrodes), L is the channel

length (i.e., the distance between the source and drain electrode). In the saturation regime, the field-effect mobility can easily be derived by fitting a linear to the square root of the drain current which is plotted against the gate voltage in the saturation regime.[4,16–18] To obtain the values presented, a fitting window of at least 10 V, containing at least 20 measured values, was used. In the saturation regime, the mobility was independent of the gate voltage.

Received: June 8, 2011
Revised: August 11, 2011
Published online: November 10, 2011

[1] J. Shinar, R. Shinar, *J. Phys. D: Appl. Phys.* **2008**, *41*, 133001.
[2] C. Dimitrakopoulos, P. Malenfant, *Adv. Mater.* **2002**, *14*, 99–117.
[3] C. D. Sheraw, L. Zhou, J. R. Huang, D. J. Gundlach, T. N. Jackson, M. G. Kane, I. G. Hill, M. S. Hammond, J. Campi, B. K. Greening, J. Francl, J. West, *Appl. Phys. Lett.* **2002**, *80*, 1088–1090.
[4] Y. Sun, Y. Liu, D. Zhu, *J. Mater. Chem*. **2005**, *15*, 53–65.
[5] C. R. Newman, C. D. Frisbie, D. A. da Silva Filho, J.-L. Brédas, P. C. Ewbank, K. R. Mann, *Chem. Mater.* **2004**, *16*, 4436–4451.
[6] S.-S. Cheng, C.-Y. Yang, C.-W. Ou, Y.-C. Chuang, M.-C. Wu, C.-W. Chub, *J. Appl. Phys.* **2008**, *103*, 094519.
[7] S. A. DiBenedetto, D. Frattarelli, A. Facchettixy, M. A. Ratner, T. J. Marks, *J. Am. Chem. Soc.* **2008**, *130*, 7528–7529.
[8] D. J. Gundlach, C.-C. S. Kuo, C. D. Sheraw, J. A. Nichols, T. N. Jackson, *Proc. SPIE* **2001**, *54*, 4466.
[9] D. S. Park, S. J. Kang, H. J. Kim, M. H. Jang, M. Noh, K.-H. Yoo, C. N. Whang, *J. Vac. Sci. Technol. B* **2005**, *23*, 926–929.
[10] C. Effertz, M. Beigmohamadi, P. Niyamakom, P. Schulz, M. Wuttig, *Phys. Status Solidi B* **2008**, *245*, 782–878.
[11] A. Ulman, *Chem. Rev.* **1996**, *96*, 1533–1554.
[12] M. Beigmohamadi, P. Niyamakom, A. Farahzadi, C. Effertz, S. Kremers, D. Brueggemann, M. Wuttig, *J. Appl. Phys.* **2008**, *104*, 013505.
[13] S. A. DiBenedetto, A. Facchetti, M. A. Ratner, T. J. Marks, *Adv. Mater.* **2009**, *21*, 1407–1433.
[14] D. Y. Kwok, A. W. Neumann, *Adv. Colloid Interface Sci.* **1999**, *81*, 167–249.
[15] J. Isrealachvili, *Intermolecular and Surface Forces*, 6th ed., Academic Press, New York **1997**.
[16] V. Coropceanu, J. Cornil, D. A. da Silva Filho, Y. Olivier, R. Silbey, J. L. Brédas, *Chem. Rev.* **2007**, *107*, 926–952.
[17] G. Horowitz, *Adv. Mater.* **1998**, *10*, 365–377.
[18] G. Horowitz, P. Delannoy, *J. Appl. Phys.* **1991**, *70*, 469–475.
[19] G. Gu, M. G. Kane, S.-C. Mau, *Appl. Phys. Lett.* **2007**, *87*, 243512.
[20] G. Gu, M. G. Kane, J. E. Doty, A. H. Firester, *Appl. Phys. Lett.* **2005**, *101*, 014504.
[21] J. Lee, J. H. Kim, S. Im, D.-Y. Jung, *J. Appl. Phys.* **2004**, *96*, 2301.